Universidad del País Vasco
Euskal Herriko Unibertsitatea
ZIENTZIA ETA TEKNOLOGIA FAKULTATEA
FACULTAD DE CIENCIA Y TECNOLOGÍA

Gradu Amaierako Lana / Trabajo Fin de Grado
Fisikako Gradua / Grado en Física

Exploring the Effects of Quantum Fluctuations in the Waveguide Expansion of a Bose-Einstein Condensate by means of Numerical Simulations

Egilea/Autora:
Maia Aguirre
Zuzendaria/Director:
Michele Modugno
Zuzendarikidea/Co-director:
Joanes Lizarraga

Leioa, 2020ko irailaren 3a /Leioa, 3 de septiembre de 2020

Abstract

In this work, we have studied a dilute and ultracold bosonic gas of weakly interacting atoms, i.e. a Bose-Einstein Condensate (BEC) by means of the Modified Gross-Pitaevskii equation (MGPE) taking into account beyond-mean-field corrections due to quantum fluctuations. We have considered the case where the cloud of atoms is strongly confined transversally (within a cigar-shaped trap) and therefore, the three-dimensional (3D) MGPE is reduced to an effective one-dimensional (1D) form by averaging over the transverse coordinates. Based on this approach, we have performed numerical simulations for analyzing the behavior of the BEC under the influence of quantum fluctuations, which give rise to an additional nonlinear quartic term. After reviewing the mathematical theory of Bose-Einstein condensation based on the GPE and the numerical methods used to integrate it we discuss the computation of the ground state and the simulation of its dynamic evolution in a waveguide (free expansion).

Contents

Introduction

The discovery of the quantum nature of matter and energy is arguably one of the most profound achievements of science in the 20^{th} century, providing a complete new perspective of our world. Fascinating as it is, Quantum Mechanics is utterly counter intuitive for observers like us, tethered to the classical realm. Moreover, direct observation of quantum properties at the microscopic level is notoriously difficult and requires very advanced experimental technology. Nevertheless, there are a few, precious examples of macroscopic systems that manifest quantum behavior such as: superfluidity, superconductivity, lasers, quantum Hall effect, giant magneto resistance, topological order and quantum-gases, in particular Bose-Einstein Condensates (BEC) [1]. As a matter of fact, a handful of Nobel prizes in physics have lately been awarded to researchers in these fields.

In this work we study a model of one such BEC system and analyze the macroscopic quantum properties it manifests.

Briefly stated, a BEC is a macroscopic state of matter (also known as the 5^{th} state of matter) which is achieved when a low density gas of identical of bosons is cooled to temperatures very close to absolute zero (-273.15° C) [2]. This cooling down is achieved by slowing down the particles; to this end the so called laser cooling and evaporative cooling methods are used [3]. As a result, the associated wavelengths of the particles that form the condensate acquire macroscopic extent.

Bosons are one of the two types of elementary particles in nature (the other type being fermions). They comprise the force carrying particles and their other salient feature is that their spin possesses an integer value. By means of the spin-statistic theorem we know that this condition makes them obey the Bose-Einstein statistic and exempts them from following Pauli's exclusion principle which in turn allows all the bosons to occupy the same quantum state.

Under such thermal conditions, a large fraction of bosons will occupy the lowest quantum state, so that the whole group starts behaving as though it were a single atom at which point microscopic quantum phenomena become apparent macroscopically [2, 4].

In BECs the quantum probability distribution given by the wave function becomes, indeed, a matter distribution of the atoms that form the condensate; this enables the direct measurement of these quantum phenomena, normally by optical means [2].

The ground state of a quantum system of identical bosons is usually described by the Gross-Pitaevskii mean-field equation (GPE). The main objective of this thesis is to study the influence of a quantum fluctuation term on the waveguide expansion of a BEC; this study will be advanced by means of numerical simulations of a MGPE.

The organization of this thesis

The present work is organized as follows: in Chapter 1 a short review about the discovery and progress of BECs is presented; in Chapter 2 we discuss the basic theory of BEC in the mean field regime (i.e., the Gross-Pitaevskii theory) and how it is modified by the addition of a quantum fluctuation term. Next, in Chapter 3 we study numerically the ground state configuration of the system and how it evolves in the waveguide after the removal of the axial confinement. Final considerations will be drawn in the Conclusions section. In the Appendix the numerical methods used for solving our MGPE are briefly discussed.

Chapter 1

Bose-Einstein Condensates: Brief History and State of the Art

One of the earliest physics lessons we are taught is that by modifying the temperature and/or pressure conditions of any substance, dramatically different states of matter can be revealed. The variation of these physical magnitudes we handle is usually at the human scale. The fascinating fact is that this is only the beginning: with further cooling, additional states of matter can eventually appear.

In fact, the approach to the coldest temperatures has paved the way for a number of striking discoveries; reaching the kelvin range uncovered superconductivity in 1911 and superfluidity in ^{4}He in 1938, whereas, achieving the millikelvin regime revealed superfluidity of ^{3}He in 1972. Cooling beyond these temperatures came hand in hand with the invention of laser cooling in the 1980s, opening up a new approach to ultra low temperature physics; studies of ultracold collisions have been made using microkelvin samples of dilute atom clouds and in order to study quantum-degenerate gases, such as Bose-Einstein condensates, nanokelvin temperatures were necessary [5]. This last achievement was first accomplished in 1995 and along with the rest of the discoveries represented significant advances in science, all of them being recognized with Nobel Prize awards in Physics. Let's rewind some decades to review how the theory of BECs was build.

Satyendra Nath Bose (1894–1974) published a paper describing the statistical nature of light in 1924 [6]. Using Bose's paper, Albert Einstein (1879–1955) predicted that a phase transition

could occur in a gas of non-interacting atoms due to these quantum statistical effects [7]. Thus, the concepts of Bose-Einstein statistics and condensation were born: a macroscopic number of non-interacting bosons can simultaneously occupy the quantum state of lowest energy [8].

Although Einstein carried out his work for non-interacting bosons, the idea can be readily extended to a system of interacting bosons. The de Broglie wavelength λ_{dB} is inversely proportional to the temperature T and therefore increases while the temperature decreases: $\lambda_{\mathrm{dB}} = \hbar/\sqrt{2mk_{\mathrm{B}}T}$. At high temperatures, the de Broglie wavelength is small compared to the spacing between atoms and the dilute gas behaves classically [5]. Hence, when a critical temperature T_{C} is reached, the wavelength λ_{dB} becomes comparable to the average inter-particle spacing and the atomic wave packets overlap [3], the system enters the quantum degeneracy regime (where the fact that particles are identical directly affects their statistical properties) and the gas becomes a "quantum soup" of indistinguishable particles [5]. In this situation, the particles behave coherently as a unique giant atom and a BEC is formed [3].

Though, Einstein's prediction did not receive much attention until Fritz London (1900–1954) suggested in 1938 that the superfluidity of ^{4}He is related to the Bose-Einstein condensation and to the existence of a macroscopic wave function for the Bose condensate [9, 10].

In 1947, by developing the idea of London, Nikolái Bogoliúbov (1909–1992) calculated the quantum depletion for a uniform weakly-interacting Bose gas [11].

Some years later, it was found experimentally that due to the strong interaction of the helium atoms, less than 10% of the superfluid ^{4}He is in the condensate state [3]. Further research had to be done to find BECs with higher occupancy and physicists started to search for weakly interacting systems of Bose gases. This was an altogether challenging task because most substances become solid or liquid at the phase transition temperature of the BEC [3].

In 1980, spin-polarized hydrogen gases, that in 1959 were proved to remain gaseous even at 0 K by Charles Hecht [12], were realized by Silvera and Walraven [13]. However, all the attempts to observe those BECs experimentally failed [3].

As we stated before, laser cooling was developed shortly after; alkali atoms turned to be very appropriate candidates for BEC experiments as they are well-suited to this laser-based method [3] due to their favorable internal energy-level structure [14].

Bose-Einstein condensation was observed in 1995 in a remarkable series of experiments on

vapours of rubidium and sodium [14]. The first BEC of dilute ^{87}Rb gases was achieved by E. Cornell and C. Wieman's [15] and four months later, two successful experimental observations of BEC, with ^{23}Na by Ketterle's group [16] and ^{7}Li by Hulet's group [17] were announced.

In each of these experiments, the atoms were confined in magnetic traps and cooled down to a scale of fractions of microkelvins by combining the advanced laser cooling (whereby the alkali gas can be cooled down to several μK) and the evaporative cooling (which can further reach down to the 50–100 nK range) techniques together [3]. Velocity-distributions showed the first indications of the Bose-Einstein condensation: the atoms produced the signature spike in velocity of the condensate once the magnetic trap was turned off [7]. In 1998, atomic condensate of hydrogen was finally realized [18].

The natural starting point for studying the behavior of the Bose-Einstein condensates, which nowadays are routinely produced with ultracold and dilute alkali-metal atoms [19], is the theory of weakly interacting bosons that takes the form of the Gross-Pitaevskii theory for inhomogeneous systems [14].

This theory was born in 1961 when Eugene P. Gross (1926–1991) and Lev Petrovich Pitaevskii (1933–) derived the mean-field equation for the space-dependent macroscopic wave function of a weakly-interacting Bose gas in the presence of an external trapping potential [20, 21]. They came up with the Gross–Pitaevskii equation, that describes the ground state of a quantum system of identical bosons: in point of fact it is a many-body nonlinear Schrödinger equation for the macroscopic wave functions. The GPE includes a term for the trap potential as well as the mean field interaction between atoms in the gas which manifests as a nonlinear term [7].

We will delve deeper into the study of the GP theory in Chapter 2 but for the moment, let us outline some of the most relevant features of these trapped Bose gases. First of all, the particle density at the center of the condensed atomic cloud is typically around $10^{13} - 10^{15}\,\mathrm{cm}^{-3}$ which is very small (consider that the density of air at standard temperature and pressure is of the order of $10^{19}\,\mathrm{cm}^{-3}$) and the temperature must be of the order of $10^{-5}\,\mathrm{K}$ or lower [4]. The total number of particles in the experiments ranges typically from a few thousands to several millions [14].

Chapter 2

The Gross-Pitaevskii Theory

In this chapter we will give an accurate mathematical description of BECs in order to be able to study the influence of the term originating from quantum fluctuations added to the regular GPE.

2.1 Mean-field approximation

The following discussion is based upon Refs. [3, 4, 14, 22].

2.1.1 General description of a BEC: the many-body systems

We are interested in studying an ultracold dilute bosonic gas confined in an external magnetic trap, which is the case for most of the BEC experiments. The confining potential of a typical magnetic trap for alkali atoms has the quadratic form characteristic of an harmonic oscillator potential [14]

$$V_{\text{ext}}(\boldsymbol{r}) = \frac{1}{2}m(\omega_x^2\, x^2 + \omega_y^2\, y^2 + \omega_z^2\, z^2). \tag{2.1}$$

In order to simplify the present discussion we will start by considering a time independent system of N identical bosons. We will also, for the moment, neglect the boson-boson interaction. The total Hamiltonian for the N particles is

$$H = \sum_{i=1}^{N} \left(\frac{-\hbar^2}{2m}\nabla_i^2 + V_{\text{ext}}(\boldsymbol{r}_i) \right), \tag{2.2}$$

whose eigenvalues have the form

$$\varepsilon_{n_x\, n_y\, n_z} = \hbar\omega_x \left(n_x + \frac{1}{2}\right) + \hbar\omega_y \left(n_y + \frac{1}{2}\right) + \hbar\omega_z \left(n_z + \frac{1}{2}\right) \tag{2.3}$$

n_x, n_y, n_z being non-negative integers.

As stated before, due to the intrinsically quantum nature of a BEC its mathematical description must be made in terms of wave functions. Therefore, the system under scrutiny can be described as a many body wave function of the form $\Psi_N(\boldsymbol{r}_1, \boldsymbol{r}_2, ...\boldsymbol{r}_N)$ where the $\boldsymbol{r}_i$ represent the spatial coordinates of each of the N bosons that form the system. The system being composed of identical bosons, the wave function must be completely symmetric with respect to the interchange of any two particles, $\boldsymbol{r}_i \leftrightarrow \boldsymbol{r}_j$ [4].

For a BEC, all particles occupy the same quantum state and for this reason we can formally take the Hartree ansatz for the many body wave function [3] so it can be written, approximately, as a product of single-particle states that fulfill the symmetry conditions.

If the system is in thermal equilibrium, at temperature T the total number of particles is given, in the grand canonical ensemble, by the sum [14]:

$$N = \sum_{n_x\, n_y\, n_z} \frac{1}{e^{\beta(\varepsilon_{n_x\, n_y\, n_z} - \mu)} - 1}, \tag{2.4}$$

where μ is the chemical potential, N is the total number of bosons, $\beta = 1/(k_{\mathrm{B}}T)$ and k_{B} is Boltzmann's constant. As we stated before, the Bose-Einstein distribution predicts a phase transition at a temperature T_{C} below which the lowest quantum state becomes macroscopically occupied and this corresponds to the onset of Bose-Einstein condensation [14]. According to equation (2.4), at $T = 0$ all the particles will be in their lowest single-particle state, so that many body wave function of the ground state $\Psi_N(\boldsymbol{r}_1, \boldsymbol{r}_2, ...\boldsymbol{r}_N)$ of N noninteracting bosons becomes [14]:

$$\Psi_N(\boldsymbol{r}_1, \boldsymbol{r}_2, ...\boldsymbol{r}_N) = \prod_{i=1}^{N} \Phi_0(\boldsymbol{r}_i), \tag{2.5}$$

where the function Φ_0 is given by

$$\Phi_0(\boldsymbol{r}) = \left(\frac{m\omega_{\mathrm{ho}}}{\pi\hbar}\right)^{3/4} e^{-\frac{m}{2\hbar}(\omega_x\, x^2 + \omega_y\, y^2 + \omega_z\, z^2)} \tag{2.6}$$

and will from now on be described as the condensate's wave function occupied by N_0 particles, with the normalization condition [3]

$$\int_{\mathbb{R}^3} |\Phi_0(\boldsymbol{r})|^2 \mathrm{d}\boldsymbol{r} = 1. \tag{2.7}$$

Thus, the wave function for the whole condensate becomes

$$\psi(\boldsymbol{r}) \equiv \sqrt{N_0}\,\Phi_0(\boldsymbol{r}), \tag{2.8}$$

which is simply the single-particle wave function normalized according to the total number of particles

$$\int_{\mathbb{R}^3} |\psi(\boldsymbol{r})|^2 \mathrm{d}\boldsymbol{r} = N. \tag{2.9}$$

Note that in the work domain covered by this research all atoms are considered to be condensated and thus, $N = N_0$. Equation (2.8) is the macroscopic wave function of the condensate. Let us recall that for the moment we are using the so called mean field approximation, where quantum and thermal fluctuation terms are neglected for being small compared to the macroscopic occupation of the condensate [4].

The density distribution then becomes

$$n(\boldsymbol{r}) = |\psi(\boldsymbol{r})|^2 \tag{2.10}$$

and its value grows with N. Instead, the size of the cloud is independent of N and is fixed by the harmonic oscillator length

$$a_{\mathrm{ho}} = \sqrt{\frac{\hbar}{m\,\omega_{\mathrm{ho}}}}, \tag{2.11}$$

which corresponds to the average width of the Gaussian wave function Φ_0 (2.6) and ω_{ho} is the geometric average of the oscillator frequencies:

$$\omega_{\mathrm{ho}} = \sqrt[3]{\omega_x\,\omega_y\,\omega_z}. \tag{2.12}$$

Therefore, the trapping frequency ω_{ho} provides an indirect measurement of a_{ho}, the first important length scale of the system which, in the samples available, has a value on the order of a few microns [14].

This length scale a_{ho} is the one that characterizes the size of a non-interacting system. In the presence of repulsive interactions, the system size is increased further by the effect of repulsive two-body forces, that make the trapped gases become almost "macroscopic" objects ("mesoscopic", as a matter of fact). Typical density variations in a condensate occur on the length scale of few microns, and are directly measurable with optical methods.

2.1.2 The effective interaction

We have developed the previous discussion considering the approximation of non-interacting bosons. In this section, we will try to make a more faithful approach to the real condensates; we will add to the description of our BECs the effect of the binary interatomic interactions at low temperatures. In fact, despite the very dilute nature of these gases the harmonic trapping greatly enhances the effects of the atom-atom interactions on important measurable quantities [14].

In order to describe the interaction between two atoms in a dilute gas only one relevant variable needs to be taken into account, namely, their relative coordinate $\boldsymbol{r}_{ij} = \boldsymbol{r}_i - \boldsymbol{r}_j$. We will therefore describe the boson-boson isotropic interaction by a potential $V_{\text{int}}(r_{ij})$ that solely depends on the distance $r_{ij} = |\boldsymbol{r}_{ij}|$ between the two atoms [4].

Hence, the many body Hamiltonian for N identical bosons held in a trap can be written as [19, 23]

$$H_N = \sum_{i=1}^{N} \left(-\frac{\hbar^2}{2m} \nabla_i^2 + V_{\text{ext}}(\boldsymbol{r}_i) \right) + \sum_{1 \leq i < j \leq N} V_{\text{int}}(r_{ij}), \tag{2.13}$$

where the $\boldsymbol{r}_i$ denote the positions of the particles, m is the mass of a boson, $V(\boldsymbol{r}_i)$ is the external trapping potential, and as explained before $V_{\text{int}}(r)$ stands for the interatomic two body interactions [3].

However, when sufficiently low energies are reached the scattering of a particle by a potential can be accurately described by a single physical parameter, the $s-$wave scattering length a_s of the potential [14]. Since we are considering the lowest energy case it seems a reasonable assumption to restrict ourselves to $s-$wave scattering ($l = 0$) and neglect the rest of the terms.

The cost of solving the above many body system increases quadratically as N grows large due to the binary interaction term. To simplify the interaction, the true interatomic potential of the binary interaction, $V_{\text{int}}(|\boldsymbol{r}_{ij}|)$, can be well approximated by a mean-field potential. This effective interacting pseudopotential has the form of a Dirac distribution at the origin [3]:

$$V_{\text{int}}(|\boldsymbol{r}_i - \boldsymbol{r}_j|) = g\, \delta(|\boldsymbol{r}_i - \boldsymbol{r}_j|), \tag{2.14}$$

where the constant $g = 4\pi\hbar^2 a_s/m$. Here a_s is the $s-$wave scattering length of the bosons (positive for repulsive interaction and negative for attractive interaction). The above approximation

(2.14) is valid because we have assumed that the system is very dilute and such that the scattering length and the range of the interatomic interaction are much smaller than the average interatomic distance [11]. Thus, the mean interaction energy of the many body system is given by:

$$\langle E_{\text{int}} \rangle = \frac{1}{2} \frac{4\pi\hbar^2 a_s}{m} \sum_{ij} |\Psi(r_{ij} \to 0)|^2, \tag{2.15}$$

where Ψ is the many body wave function and $r_{ij} \to 0$ means that the separation between the two atoms of the condensate is very small compared to the average distance between particles $d \equiv v^{1/3} = (V/N)^{1/3}$ [19] and to the de Broglie wavelength λ_{dB}, but as stated before, large compared to a_s. An equivalent statement is that $|\Psi|^2$ should be understood as averaged over a volume $\gg a_s^3$ [19]. This leaves us with several conditions that must be fulfilled for (2.15) to be valid. First, we require that $d \gg a_s$ which generally holds due to the diluteness of the gas. Second, $\lambda_{\text{dB}} \gg a_s$ will enable us to take into account the averaged effect of the potential. This is a physically important restriction because in quantum mechanics particles cannot be localized and one must consider a region of space comparable in size to their thermal wavelength, namely, the region of space where it is highly probable to find them. Therefore, the particles will experience an averaged effect of the potential. This last condition must hold to the first order in a_s neglecting the $l \neq 0$ scattering.

If we write equation (2.15) in terms of the many body wave function, adding the interaction between every pair of atoms in the condensate and neglecting three particle interactions and quantum depletion terms we get:

$$\langle E_{\text{int}} \rangle = \frac{1}{2} \frac{4\pi\hbar^2\, a_s}{m} \sum_{ij} \int_{\mathbb{R}^3} |\Phi(\boldsymbol{r})|^4 \mathrm{d}\boldsymbol{r} = \frac{1}{2} \frac{4\pi\hbar^2\, a_s}{m} N(N-1) \int_{\mathbb{R}^3} |\Phi(\boldsymbol{r})|^4 \mathrm{d}\boldsymbol{r}. \tag{2.16}$$

Importantly, here and in equation (2.15) a $1/2$ factor arises in order to count each interaction between particle i and particle j only once and not twice. Then the energy of the state (2.5) can be written as

$$E = N \int_{\mathbb{R}^3} \left[\frac{\hbar^2}{2m} |\nabla \Phi_0(\boldsymbol{r})|^2 + V(\boldsymbol{r}) |\Phi_0(\boldsymbol{r})|^2 + \frac{N-1}{2} g\, |\Phi_0(\boldsymbol{r})|^4 \right] \mathrm{d}\boldsymbol{r}. \tag{2.17}$$

This description of the ground state of a quantum system of identical bosons using the Hartree-Fock approximation and the pseudopotential interaction model is called the Gross–Pitaevskii equation and equation (2.17) is the well-known Gross-Pitaevskii energy functional. The Gross-Pitaevskii equation governing the motion of the condensate is obtained by functional derivation

[24]. So,

$$\imath\,\hbar\,\partial_t\psi(\boldsymbol{r},t) = \frac{\delta E(\psi)}{\delta\psi^*} = \left[-\frac{\hbar^2}{2m}\,\nabla^2 + V(\boldsymbol{r}) + g\,|\psi(\boldsymbol{r},t)|^2\right]\,\psi(\boldsymbol{r},t), \tag{2.18}$$

where ψ^* denotes the complex conjugate of $\psi(\boldsymbol{r},t)$. Notice that in (2.18) we used the normalized wave function according to the total number of the particles. We obtained a nonlinear Schrödinger equation (NLSE) with cubic nonlinearity.

Henceforth, we will not be studying the GPE equation but a Modified GPE equation with an additional correction term to take into account the quantum fluctuations that occur in BECs.

2.2 Beyond the mean-field approximation

We have decided to go beyond the mean field approximation by taking into account the quantum depletion effect of the condensate. In order to complete this undertaking we need to come up with a new term able to accurately account for this correction to the mean-field approximation. This new term represents the fraction of atoms which –because of correlation effects– do not occupy the condensate at zero temperature. As we stated before, the quantum depletion is ignored in the derivation of the Gross-Pitaevskii equation. Therefore, it is useful to have a reliable estimate of the magnitude of the correction in order to check the validity of the Gross-Pitaevskii theory. In the presently available experimental conditions, the effect of the quantum depletion of the condensate is very small (less than 1%) [14]. We will numerically work out these effects in Chapter 3 in an attempt to validate the Gross-Pitaevskii theory with the calculated results.

Quantum corrections to density $n(\boldsymbol{r})$ (equation (2.10)) are dominated by quantum fluctuations with wavelengths of order $1/\sqrt{n(\boldsymbol{r})\,a_s}$, where a_s is the so far well known $s-$wave scattering length. By expanding the equations for the Hartree-Fock approximation to second order in the gradient expansion, we derive local correction terms to the Gross-Pitaevskii equation that take into account the dominant effects of quantum fluctuations. By carrying out a self-consistent one-loop calculation through second order in the gradient expansion, we determine the correction terms that must be added to the Gross-Pitaevskii equation (2.18) to take into account the effects of quantum fluctuations [25]. We obtain the MGPE for any arbitrary potential [26]:

$$\imath\,\hbar\,\partial_t\psi(\boldsymbol{r},t) = \left[-\frac{\hbar^2}{2m}\,\nabla^2 + V(\boldsymbol{r}) + g_{3\mathrm{D}}\,|\psi(\boldsymbol{r},t)|^2 + g'_{3\mathrm{D}}\,|\psi(\boldsymbol{r},t)|^3\right]\,\psi(\boldsymbol{r},t), \tag{2.19}$$

where we tagged $g'_{3\mathrm{D}}$ the term corresponding to the quantum depletion that is defined as:

$$g'_{3\mathrm{D}} = \frac{128}{3}\,\frac{\hbar}{m\omega_{\mathrm{ho}}}\,\sqrt{a_s^5\,\pi} \tag{2.20}$$

and we renamed our previous g term as $g_{3\mathrm{D}}$.

2.3 The Modified Gross-Pitaevskii Equation

This section follows the approaches made in Refs [27] and [28] and will be centered on how to re-write the MGPE (2.19) in order to ease its numerical solution. With that purpose we will start re-scaling the equation to express it with the help of dimensionless variables. Then, we will factorize the three-dimensional wave equation into a transverse and a longitudinal component to obtain a one-dimensional version of the MGPE. Finally, we will spell out how to deal with the time dependence.

2.3.1 Dimensionless form of the MGPE

We are considering the case of a cigar-shaped trap, viz. a tight transverse confinement whereby the applied external potential has cylindrical symmetry. Specifically, we will analyze a harmonic trapping potential split into two pieces, the first transversal, describing the trapping along the transverse dimensions; the second longitudinal, i.e. dependant on the z coordinate. The latter piece describes the longitudinal trapping, which is much weaker than the transversal one (the $\omega_z/\omega_\perp < 1$ inequality holds in a cigar shaped trap) [28]. So,

$$V(x,y,z) = \frac{1}{2}\,m\,\omega_\perp^2\,(x^2+y^2) + \frac{1}{2}\,m\,\omega_z^2\,z^2, \tag{2.21}$$

where $\omega_\perp$ and ω_z are respectively the trap frequencies in the radial and axial directions.

Then (2.19) becomes:

$$\imath\,\hbar\,\frac{\partial\psi\,(\boldsymbol{r},t)}{\partial t} = \left[-\frac{\hbar^2}{2m}\,\nabla^2 + \frac{1}{2}\,m\,\omega_\perp^2\,\left(x^2+y^2\right) + \frac{1}{2}\,m\,\omega_\perp^2\,z^2 + \frac{4\pi\hbar^2\,a_s}{m}\,\left|\psi\,(\boldsymbol{r},t)\right|^2 + \frac{128\hbar}{3m\omega_\perp}\,\sqrt{a_s^5\pi}\,\left|\psi\,(\boldsymbol{r},t)\right|^3\right]\psi\,(\boldsymbol{r},t)\,. \tag{2.22}$$

With hindsight we claim that the numerical solution of these equations can be greatly facilitated by the device of rearranging them in an equivalent but simpler form. This scheme consists in

the rewriting of the equations in dimensionless form, by expressing lengths and energies in harmonic oscillator (ho) units. Thus, the spatial coordinates, the energy, and the wave function are rescaled as follows [29]:

$$\tilde{\boldsymbol{r}} = \frac{\boldsymbol{r}}{a_\perp} \qquad \tilde{E} = \frac{E}{\hbar\omega_\perp} \qquad \tilde{\psi} = \sqrt{\frac{a_\perp^3}{N}}\,\psi$$

where the rescaled $\tilde{\psi}$ is normalized to unity as in equation (2.8) and $a_\perp = \sqrt{\frac{\hbar}{m\,\omega_\perp}}$. The reduction to the dimensionless form results in:

$$\imath\,\frac{\partial\tilde{\psi}\,(\boldsymbol{r},t)}{\partial t} = \left[-\frac{1}{2}\,\nabla^2 + \frac{1}{2}\,\left(\tilde{x}^2+\tilde{y}^2\right) + \frac{1}{2}\,\frac{\omega_z^2}{\omega_\perp^2}\,\tilde{z}^2 + 4\pi\frac{a_s}{a_\perp}\,N\,\left|\tilde{\psi}\,(\boldsymbol{r},t)\right|^2 + \frac{128}{3}\,\sqrt{\frac{a_s^5}{a_\perp}\,\pi\,N^3}\,\left|\tilde{\psi}\,(\boldsymbol{r},t)\right|^3\right]\tilde{\psi}\,(\boldsymbol{r},t)\,. \quad (2.23)$$

2.3.2 3D to 1D reduction of the MGPE

In the following we will reduce the 3D (three dimensional) MGPE to an effective 1D (one dimensional) form by averaging over the transverse coordinates. The resultant effective equation produces results in good agreement with the original 3D formulation [29]. The 3D GPE can be obtained by using the quantum least action principle, i.e. 3D MGPE is the Euler-Lagrange equation of the following action functional

$$S = \int \mathrm{d}t\,\mathrm{d}\boldsymbol{r}\,\tilde{\psi}^*(\boldsymbol{r},t)\left[\imath\,\frac{\partial}{\partial t} + \frac{1}{2}\,\nabla^2 - \frac{1}{2}\,\left(\tilde{x}^2+\tilde{y}^2\right) - \frac{1}{2}\,\frac{\omega_z^2}{\omega_\perp^2}\,\tilde{z}^2 + 2\pi\frac{a_s}{a_\perp}\,N\,\left|\tilde{\psi}\,(\boldsymbol{r},t)\right|^2 + \frac{2}{5}\frac{128}{3}\,\sqrt{\left(\frac{a_s}{a_\perp}\right)^5\,\pi\,N^3}\,\left(\sqrt{\tilde{\psi}^*(\boldsymbol{r},t)\,\tilde{\psi}\,(\boldsymbol{r},t)}\right)^3\right]\tilde{\psi}\,(\boldsymbol{r},t)\,. \quad (2.24)$$

We want to minimize this action functional by factorizing the wave function into two components: a transversal (radial) component and a longitudinal (axial) component. A natural choice is considering the fundamental Gaussian state of the harmonic oscillator for the transverse component

$$\tilde{\psi}\,(\boldsymbol{r},t) = \frac{1}{\sqrt{\pi}\sigma}\,\exp\left[-\frac{\tilde{x}^2+\tilde{y}^2}{2\sigma^2}\right]\,\tilde{\Phi}\,(z,t) = \tilde{\Gamma}\,(x,y)\;\tilde{\Phi}\,(z,t)\,. \quad (2.25)$$

The choice of a Gaussian shape for the condensate in the transverse direction is well justified in the limit of weak interatomic coupling, because the exact ground state of the linear Schrödinger equation with harmonic potential is Gaussian [27].

Next we must determine the variational function $\tilde{\Phi}\,(z,t)$ by minimization of the action functional. With this objective in mind we will assume at this stance that the transverse wave function $\tilde{\Gamma}$

showcases a much slower variation along the axial direction than with respect to the transverse directions:

$$\nabla^2\tilde{\psi}\left(\boldsymbol{r},t\right)=\tilde{\Gamma}\left(x,y\right)\,\frac{\partial^2\tilde{\Phi}\left(z,t\right)}{\partial z^2}+\tilde{\Phi}\left(z,t\right)\,\left(\frac{\partial^2}{\partial x^2}+\frac{\partial^2}{\partial y^2}\right)\,\tilde{\Gamma}\left(x,y\right). \tag{2.26}$$

By inserting the trial wave-function in (2.23) and after spatial integration over the transverse coordinates the action functional becomes

$$\begin{aligned}S=\int \mathrm{d}t\,\mathrm{d}z\,\tilde{\Phi}^*(z,t)\Bigg[\imath\,\frac{\partial}{\partial t}+\frac{1}{2}\frac{\partial^2\tilde{\Phi}\left(z,t\right)}{\partial z^2}-\frac{1}{2}\frac{\omega_z^2}{\omega_\perp^2}\tilde{z}^2-\frac{a_s}{a_\perp}\frac{N}{\sigma^2}\left|\tilde{\Phi}\left(z,t\right)\right|^2\\ -\frac{512}{75}\frac{\sqrt{\left(\frac{a_s}{a_\perp}\right)^5N^3}}{\pi\sigma^2\left|\sigma\right|}\,\tilde{\Phi}^*(z,t)\,\tilde{\Phi}\left(z,t\right)\sqrt{\tilde{\Phi}^*(z,t)\,\tilde{\Phi}\left(z,t\right)}\Bigg]\,\tilde{\Phi}\left(z,t\right).\end{aligned} \tag{2.27}$$

In the process of doing the calculation, it is also necessary to use the adiabatic approximation, which consists of neglecting the spatial derivatives of the transverse width, i.e. we assume that σ is constant:

$$\sigma^2=\frac{\hbar}{m\omega_z}\Longleftrightarrow\tilde{\sigma}^2=\frac{\omega_\perp}{\omega_z}. \tag{2.28}$$

As a matter of fact, this is an exact result under the assumption that the transverse potential is strong enough to confine the atoms in the fundamental state.

The Euler-Lagrange equation with respect to $\tilde{\Phi}^*(z,t)$ reads:

$$\begin{aligned}\imath\,\frac{\partial}{\partial t}\tilde{\Phi}\left(z,t\right)+\frac{1}{2}\frac{\partial^2\tilde{\Phi}\left(z,t\right)}{\partial z^2}\,\tilde{\Phi}\left(z,t\right)-\frac{1}{2}\frac{\omega_z^2}{\omega_\perp^2}\tilde{z}^2\,\tilde{\Phi}\left(z,t\right)-2\frac{a_s}{a_\perp}\frac{N}{\sigma^2}\tilde{\Phi}^*(z,t)\,\tilde{\Phi}\left(z,t\right)^2\\ -\frac{5}{2}\,\frac{512}{75}\frac{\sqrt{\left(\frac{a_s}{a_\perp}\right)^5N^3}}{\pi\sigma^2\left|\sigma\right|}\tilde{\Phi}^*(z,t)^{3/2}\,\tilde{\Phi}\left(z,t\right)^{5/2}=0.\end{aligned} \tag{2.29}$$

This equation is a 1D Gross-Pitaevskii equation with an additional quartic nonlinear term which describes quantum fluctuations. This expression is the main result of this section.

It is essential noticing that the terms $g_{3\mathrm{D}}$ and $g'_{3\mathrm{D}}$ have been renormalized according to the following expressions:

$$g_{1\mathrm{D}}=\frac{mN}{2\pi\sigma^2\hbar a_\perp}\,g_{3\mathrm{D}},\qquad\qquad g'_{1\mathrm{D}}=\frac{2}{5}\sqrt{\frac{N^3}{a_\perp^9\pi^3}}\,\frac{g'_{3\mathrm{D}}}{\sigma^2|\sigma|}. \tag{2.30}$$

For the sake of notational simplicity hereafter the symbols g and g' stand for their renormalized

values

$$g = g_{1\mathrm{D}} = 2\,\frac{a_s N}{a_\perp \sigma^2}, \qquad\qquad g' = g'_{1\mathrm{D}} = \frac{256}{15}\,\frac{\sqrt{\left(\frac{a_s}{a_\perp}\right)^5 N^3}}{\pi\sigma^2|\sigma|}. \tag{2.31}$$

2.3.3 Stationary MGPE

The equation one must consider to calculate the ground state of a confined BEC is given by the following expression:

Note: below we make use of the dimensionless auxiliary quantity $\lambda = (\omega_z/\omega_\perp)^2$.

$$\left[-\frac{1}{2}\frac{\partial^2}{\partial z^2} \;+\; \frac{1}{2}\,\lambda\,\tilde{z}^2 \;+\; 2\frac{a_s}{a_\perp}\,\frac{N}{\sigma^2}\,|\tilde{\Phi}\,(z)\,|^2 \;+\; \frac{256}{15}\frac{\sqrt{\left(\frac{a_s}{a_\perp}\right)^5 N^3}}{\pi\sigma^2\,|\sigma|}\,|\tilde{\Phi}\,(z)\,|^3\right]\tilde{\Phi}\,(z) \;\;=\;\; \tilde{\mu}\,\tilde{\Phi}\,(z)\,, \tag{2.32}$$

where $\tilde{\mu} = \mu/(\hbar\omega_\perp)$ naturally stands for the normalized dimensionless chemical potential. In the next chapter we will study the influence of the nonlinear terms of the above equation; therefore it is extremely convenient to rewrite the equation in a terser form:

$$\left[-\frac{1}{2}\frac{\partial^2}{\partial z^2} + \frac{1}{2}\,\lambda\,\tilde{z}^2 + g\,|\tilde{\Phi}\,(z)\,|^2 + g'\,|\tilde{\Phi}\,(z)\,|^3\right]\tilde{\Phi}\,(z) = \tilde{\mu}\,\tilde{\Phi}\,(z) \tag{2.33}$$

such that we can focus on the effects that the g and g' coefficients may have. This equation can be interpreted as the Euler-Lagrange equation associated with the constraint minimization problem and the chemical potential plays the role of a Lagrange multiplier associated to the norm conservation.

As a consequence, we are dealing with a nonlinear eigenvalue problem and any eigenvalue $\tilde{\mu}$ can be computed from its corresponding eigenfunction $\tilde{\Phi}\,(z)$ by imposing the normalization condition [3]

$$\tilde{\mu}(\tilde{\Phi}) = \int\left[\frac{1}{2}\left|\frac{\partial\tilde{\Phi}\,(z)}{\partial z}\right|^2 + \frac{1}{2}\,\lambda\,\tilde{z}^2\,|\tilde{\Phi}\,(z)\,|^2 + \frac{g}{2}|\tilde{\Phi}\,(z)\,|^4 + \frac{2}{5}\,g'\,|\tilde{\Phi}\,(z)\,|^5\right]\,\mathrm{d}z. \tag{2.34}$$

Once the ground state solution of equation (2.32) is known we are capable of calculating the time evolution of the fundamental state of the condensates that solely depends on a phase factor:

$$\tilde{\Phi}\,(z,t) = \tilde{\Phi}\,(z)\,e^{-\imath\tilde{\mu}t}. \tag{2.35}$$

However, we are interested in studying the time evolution of the condensates once the axial trapping potential is turned off. In order to do so, the time dependent MGPE must be solved,

namely, equation (2.29) without the transverse potential term. This processes will be expounded in the next chapter.

Chapter 3

Numerical Solutions

In this chapter we will expose the guidelines followed to solve the dimensionless one-dimensional Gross-Pitaevskii equation (2.33). As we have already explained, we are intent on analyzing the behavior and general properties of the modified equation while varying the parameters that multiply the non-linear terms; thence, we expect the use of the dimensionless form of the equation to be so much more revealing.

Please note the following change of notation that we adopt from this point onward: while functions, energies, chemical potentials, coordinates, wave functions, etc. that we will be using will all be truly dimensionless quantities, for the sake of clarity we will altogether drop the tildes.

3.1 Computation of stationary states

In order to solve the MGPE numerically it is fundamental to establish the initial state of the condensate. This initial state will be obtained by reaching the ground state, which by definition is the state that minimizes the energy of the system and corresponds to the state in which the condensate is produced experimentally.

As mentioned in Chapter 2, the problem consists in finding a solution to the equation (2.33).

Thus, to reshape conveniently our wave function at each step, we need to know its energy functional and change it iteratively assuring that the new wave function will be a state of less

energy than the previous one, the energy functional being [3]:

$$E_g(\Phi) = \int_{\mathbb{R}} \left[\frac{1}{2} \left| \frac{\partial^2}{\partial z^2} \tilde{\Phi} \right|^2 + \frac{1}{2} \lambda \tilde{z}^2 |\tilde{\Phi}|^2 + \frac{g}{2} |\tilde{\Phi}|^4 + \frac{2}{5} g' |\tilde{\Phi}|^5 \right] \mathrm{d}z. \tag{3.1}$$

Summarizing, calculating the global minimal solutions Φ_g to the energy functional (3.1) corresponds to obtaining the ground state solution while local minima are excited states.

In the following we outline one of the many approaches that can be used for numerically computing Φ_g.

3.2 Approximate solution

With the object of numerically computing solutions to the minimization problem, an iterative procedure is needed. This means that an initial guess has to be given to the method in order to initialize it and then the minimization process computes a minimal solution through iterations.

For a non-rotating BEC, it can be proved that the global minimal solution is unique and gives a ground state $\Phi_g \geq 0$ for a positive initial data Φ_0 [30].

We will consider the Thomas-Fermi (TF) approximation of the ground state as initial guess with a simple harmonic oscillator as the potential [4].

3.2.1 Thomas-Fermi Regime

This approximation is based on ignoring the kinetic energy of the particles at temperatures close to zero Kelvin and will provide a very reasonable estimate of the stationary state energy of our condensate. Since the TF limit is characterized by slowly varying the density of the gas in space, the interaction term will dominate over the kinetic one enabling us to write the equation in a very simple form

$$\left[V_{\text{ext}}(z) + g \left| \Phi(z) \right|^2 \right] \Phi(z) = \mu \, \Phi(z), \tag{3.2}$$

where we are ignoring the quantum fluctuation g' term. Once again we are solely developing

the one-dimensional case whose solution is

$$\Phi(z) = \begin{cases} \sqrt{\frac{\mu - V_{\text{ext}}(z)}{g}} & \mu \geq V_{\text{ext}}(z) \\ 0 & \text{elsewhere.} \end{cases} \tag{3.3}$$

As we imposed a harmonic type of trapping external potential, we will develop the solution given above for this kind of potential.

To calculate the chemical potential we need to integrate the following equation

$$N = \int_{-R_{\text{TF}}}^{+R_{\text{TF}}} |\Phi(z)|^2 \, dz = \int_{-R_{\text{TF}}}^{+R_{\text{TF}}} \left(\frac{\mu}{g} - \frac{m\omega_z^2}{2g} z^2 \right) \mathrm{d}z, \tag{3.4}$$

where $R_{\text{TF}} = \sqrt{\mu/(m\omega_z^2)}$ is the cut-off distance of the Thomas Fermi approximation and gives the result

$$\mu(N) = \left(\frac{3}{5} N g \, \omega_z \sqrt{m} \right)^{2/3}, \tag{3.5}$$

where ω_z is the frequency of the harmonic potentials in the z direction.

The energy of our initial guess of the BEC wave-function is

$$E = \int \mu(N) \, \mathrm{d}N = \frac{3}{5} N \, \mu(N). \tag{3.6}$$

Once we have described the shape of our initial guess, we shall choose a numerical method to minimize the energy and achieve the initial state of the condensate. The initial distribution of the BEC will be calculated using the Backward Euler pseudoSpectral (BESP) scheme as we assume the initial distribution is the ground state of the system. A description of this method can be found in Appendix A.1. Consequently, once the ground state of our condensate is achieved we want to examine its time evolution. For that aim, the numerical spectral scheme used to model the dynamics of our MGPE is presented in Appendix A.2.

3.3 Results of the numerical simulations

In this section we present the numerical results of the performed simulations. To compute the ground state we have used the BESP method (Appendix A.1 [30]) in 1D with the stopping criterion set as $\Delta E < 10^{-12}$. Besides, for the time-dependent analysis we have chosen the ADI-TSSP scheme (Appendix A.2 [31]) with a time step of 10^{-3}.

3.3.1 Ground State solutions

We now proceed to study the influence of the quantum fluctuation term in the ground state solution of the BEC. For that purpose, we will calculate the numerical solution of equation (2.33) with different g and g' terms, which, as we already know, stand respectively for the cubic and quartic nonlinearities. From now on, the starting point of every simulation will be the Thomas-Fermi initial data.

Bearing in mind that the g' term is a correction to the previous terms, it can never be bigger than g. Thus, the value of the g' parameter we contemplate depends essentially on the g term. The constraint used is $g' = k \cdot g$ where $k = 0,\ 0.01,\ 0.1,\ 1$. Our convention for Figure 3.1 is:

k	Color	LineStyle
0	Green	——
0.01	Magenta	- - - -
0.1	Red	· · · ·
1	Blue	- · - ·

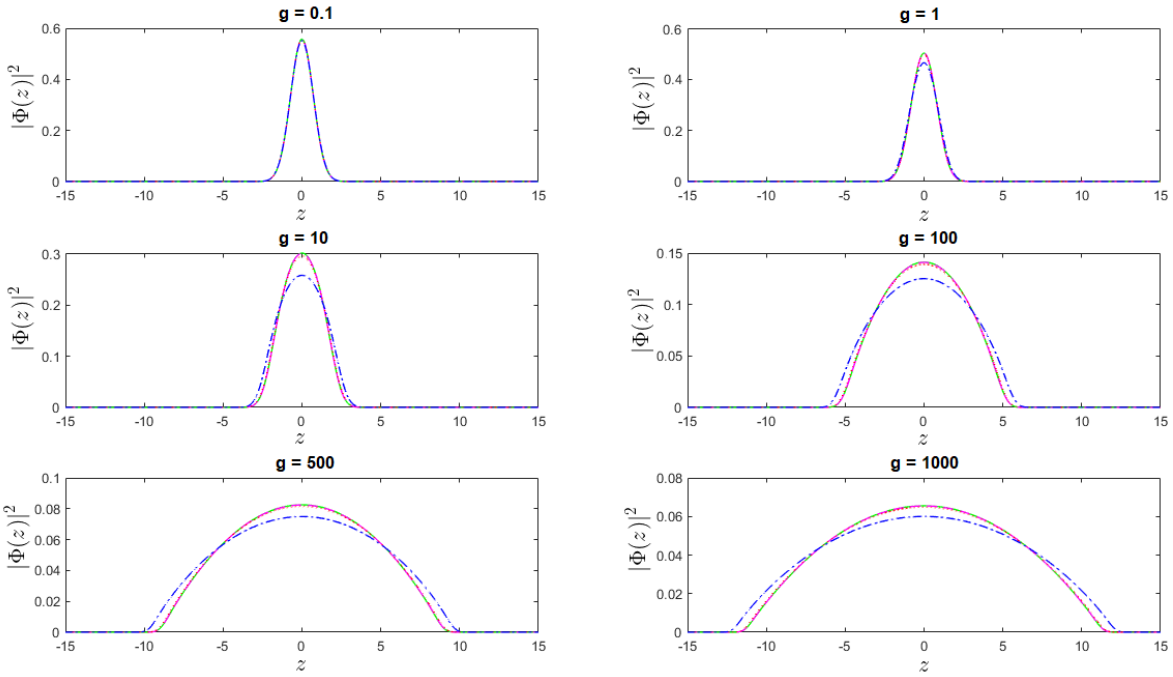

Figure 3.1: Density distribution of the ground state for different values of the parameters g and g', as obtained from the numerical solution of the MGPE.

Figure 3.1 illustrates the shape of the ground state of a BEC under the influence of specific g and g' terms. We recall that the shape of the density distribution is mainly affected by the interplay of the kinetic, potential, and mean field terms (the latter being the one proportional to g). In this respect, the term proportional to g' has to be considered a perturbation. Indeed, the g term represents the atom-atom interactions upon which the GPE is based and g' introduces the corrections due to quantum fluctuation.

Then, let us first consider the effect of g. We recall that it is proportional to Na_s

$$g = 2\frac{a_s N}{a_\perp \sigma^2}.$$

Figure 3.1 shows that the size of the system increases by increasing g (that is, the number of atoms N and/or the scattering length a_s), the shape of the density distribution going from a Gaussian profile (in the non interacting limit $g = 0$) to a TF profile in the large N and/or large a_s limit.

As for the effect that the quantum fluctuation term has, its net effect is to lower the central density, by pushing atoms out from the bulk into the tails. It is worth noticing that the influence of the g' term becomes significant, i.e. differs from the result obtained using $g' = 0$, when its value is of the order of g, that is to say, when $k = 1$. Further, from Figure 3.1 it is also discernible that the influence of the g' coefficient augments in the range $10 < g < 500$.

Likewise, by establishing $g' = 0$ we would retrieve the GPE. Let us recall the expression of g':

$$g' = \frac{256}{15}\frac{\sqrt{\left(\frac{a_s}{a_\perp}\right)^5 N^3}}{\pi\sigma^2|\sigma|}.$$

Thus, for the quantum depletion term to have an effect in the shape of the condensate $g' \approx g$ and accordingly N must be of the order

$$N \approx \left(\frac{15}{128}\right)^2 \pi^2 \sigma^2 \left(\frac{a_\perp}{a_s}\right)^3. \tag{3.7}$$

The values of the chemical potential μ for each case are:

g	$k = 0$	$k = 0.01$	$k = 0.1$	$k = 1$
0.1	0.5396	0.5398	0.5422	0.5655
1	0.8994	0.8721	0.8915	1.0711
10	3.1072	3.1169	3.2021	3.9526
100	14.1343	14.1655	14.4426	16.9545
500	41.2816	41.3514	41.9736	47.7252
1000	65.5236	65.6223	66.5033	74.7075

Table 3.1: Values of the chemical potential μ.

Again, these tabulated values sustain the conclusion that the effect of the g' term is only appreciable when $g' \approx g$.

From Figure 3.1 we can also conclude that the results calculated for the values $k = 0$ and $k = 0.01$ are barely distinguishable. Subsequently, for the numerical simulations of the dynamical evolution he case $k = 0.01$ will be omitted.

3.3.2 Solutions for the Dynamic Evolution

In order to explore the dynamic evolution of the condensates the trapping potential is removed from equation (2.29).

The next figures show qualitatively the behavior of the time evolution of the density of the BEC for $g = 0.1$ and $g = 100$. We have omitted the influence of g' because in this qualitative analysis it would not be appreciable.

The chosen waveguide in these cases (Figures 3.2, 3.3 and 3.4) has a width of 160 and we have let each system evolve up to a final time $t = 10$.

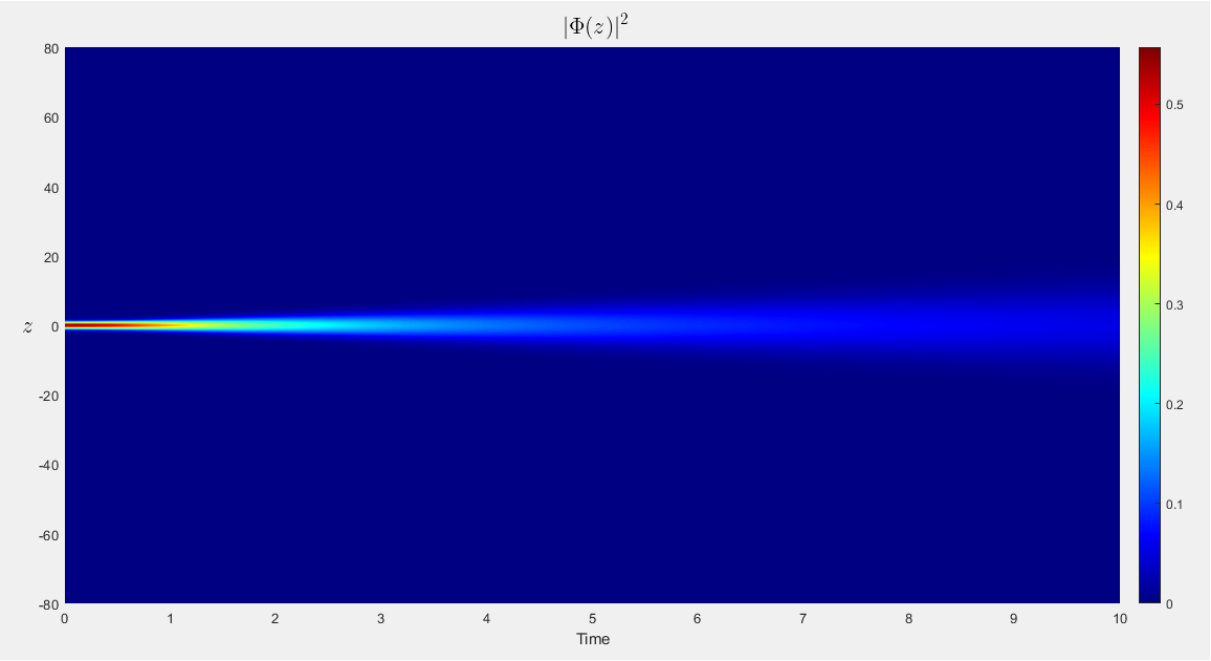

Figure 3.2: 2D representation of the time evolution of $|\Phi|^2$ with $g = 0.1$.

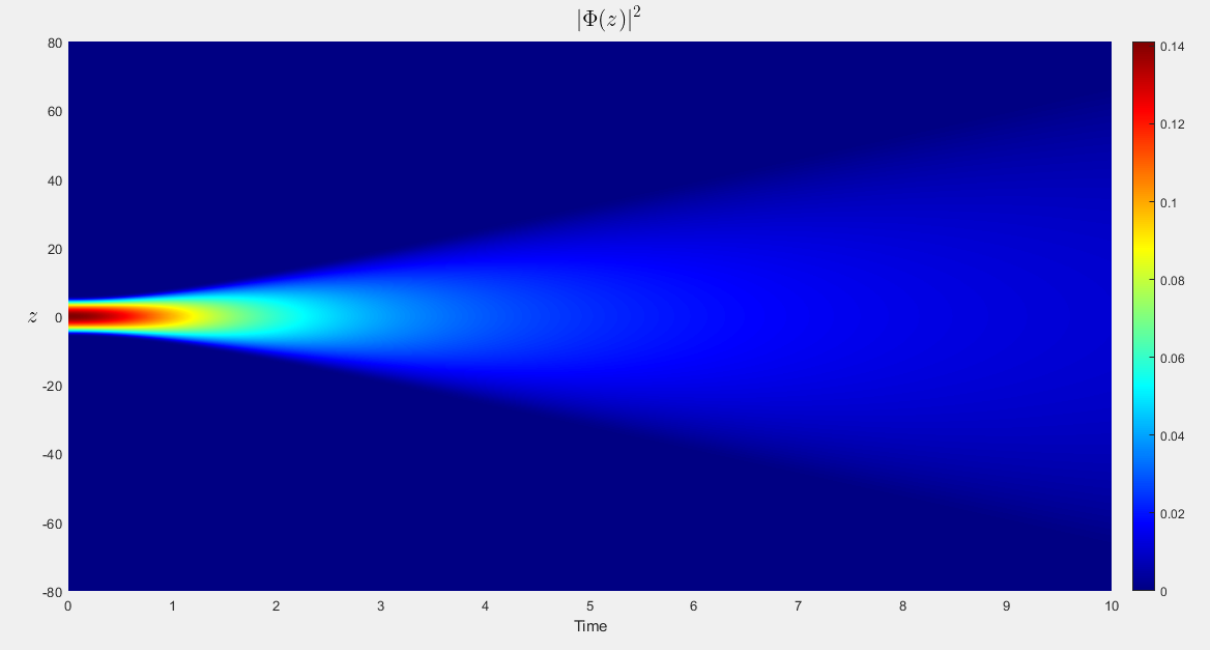

Figure 3.3: 2D representation of the time evolution of $|\Phi|^2$ with $g = 100$.

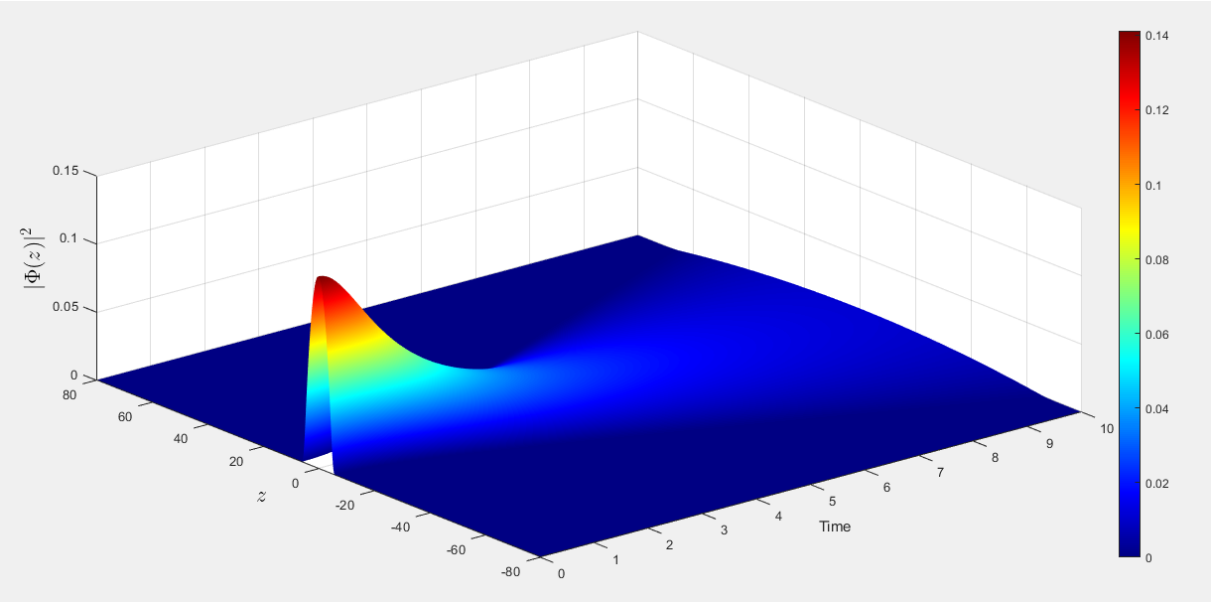

Figure 3.4: 3D representation of the time evolution of $|\Phi|^2$ with $g = 100$.

Along the same lines followed for the time-independent analysis developed in the previous section, the effect of the binary interatomic interaction described by the g term is apparent in the dynamic evolution: the greater the g term, the more interactions between particles occur and as a consequence, the wider the shape of the density distribution becomes. We observe that over time the wave function expands as a result of the removal of the trapping potential. Once again, the g term has a remarkable impact in this expansion making it substantially faster as g grows. This effect can be clearly seen by comparing Figures 3.2 and 3.3.

Furthermore, we proceed to study quantitatively the dynamic evolution of the BECs in order to determine the impact that the quantum fluctuation term may or may not have in the time-dependent MGPE.

From now on our plotting convention reads:

k	Color	LineStyle
0	Green	——
0.1	Red	· · · ·
1	Blue	- · - ·

In Figure 3.5 we show the root-mean-square (rms) value of the longitudinal (z) coordinate of

the wave function plotted as a function of time until $t = 10$.

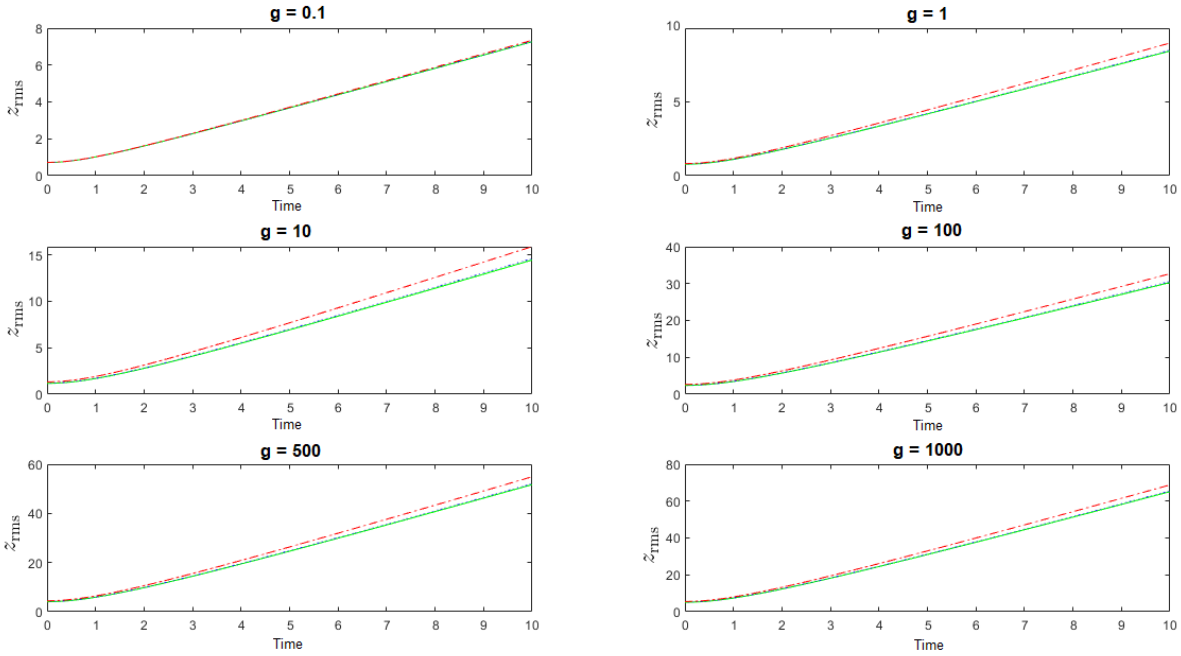

Figure 3.5: rms of z as a function of time ,for different values of the parameters g and g'.

Notice that in Figure 3.5 the vertical axis is different for each plot due to the influence of the g term. Besides, the presence of quantum fluctuations adds an expansion effect with respect to mean-field case ($g' = 0$).

Indeed, even more compelling insight can be obtained from this same analysis; to this end we will compare in the same figure the ratio of the final values at $t = 10$ of the six plots represented in Figure 3.5. That is to say, we will represent the following percentage variation,

$$\Delta[g] \equiv \frac{z_{\mathrm{rms}}[g, g']}{z_{\mathrm{rms}}[g, g' = 0]} - 1 \tag{3.8}$$

as a function of g in a logarithmic scale.

From Figure 3.6 we can conclude that the quantum fluctuation term g' has its maximum effect when $g = 10$. That maximum effect amounts to a 10% when $g' = 1$ and to a 1% when $g' = 0.1$.

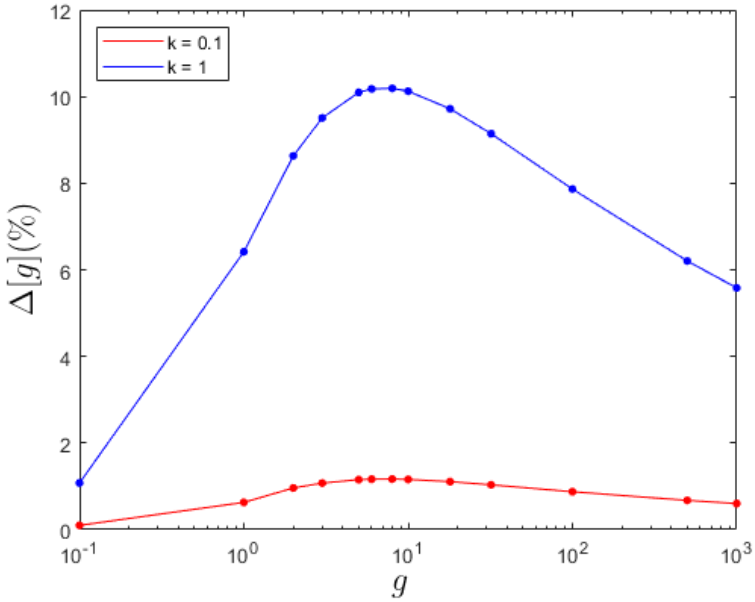

Figure 3.6: Percentage variation of the final values at $t = 10$ of $z_{\mathrm{rms}}[g, g']$ as a function of g and $g' = k \cdot g$.

In the last two figures of this chapter we will plot sections of the density distribution $|\Phi|^2$ at $t = 5$ for different values of g and g', following the procedure we have carried out so far.

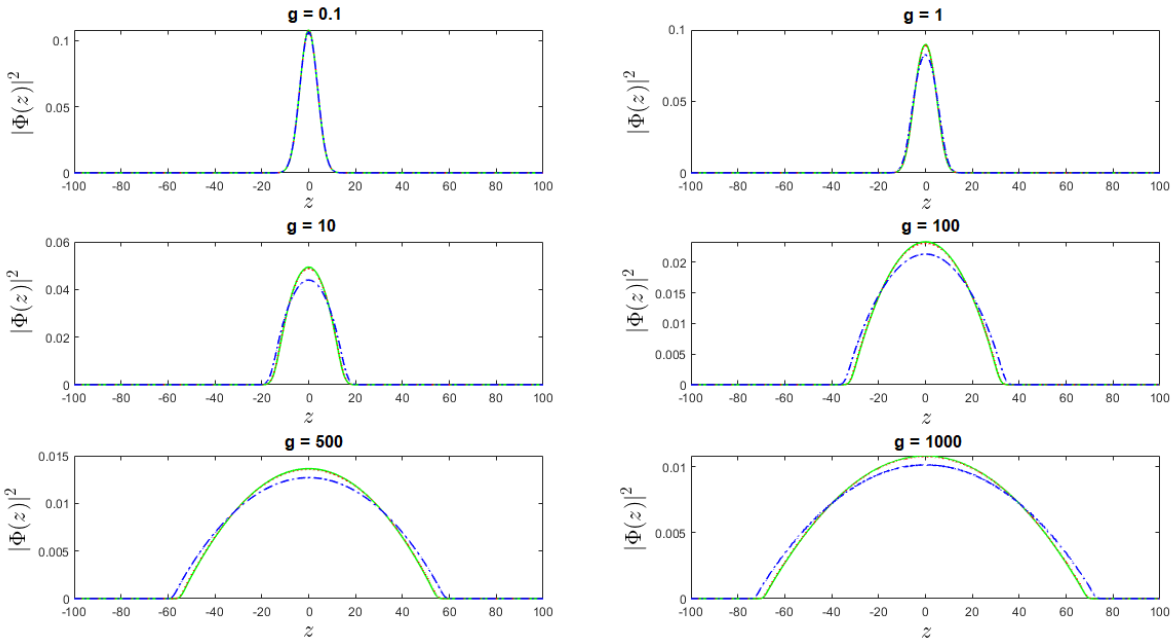

Figure 3.7: Sections of the dynamic evolution of the MGPE at $t = 5$ for different g and g' terms.

The cases $g = 0.1$, $g' = 0$ and $g = 100$, $g' = 0$ in Figure 3.7 (green continuous line) are sections of Figures 3.2 and 3.3 respectively. Consistently, once again we notice that the influence of the g' term is appreciable only when $g' \approx g$. Nevertheless, notice that in Figure 3.7 each plot has a different vertical axis and hence, the scale difference of the density distribution of the condensate as a function of g is not readily noticeable. With the purpose of showing that effect we now plot all the graphics in Figure 3.8 together.

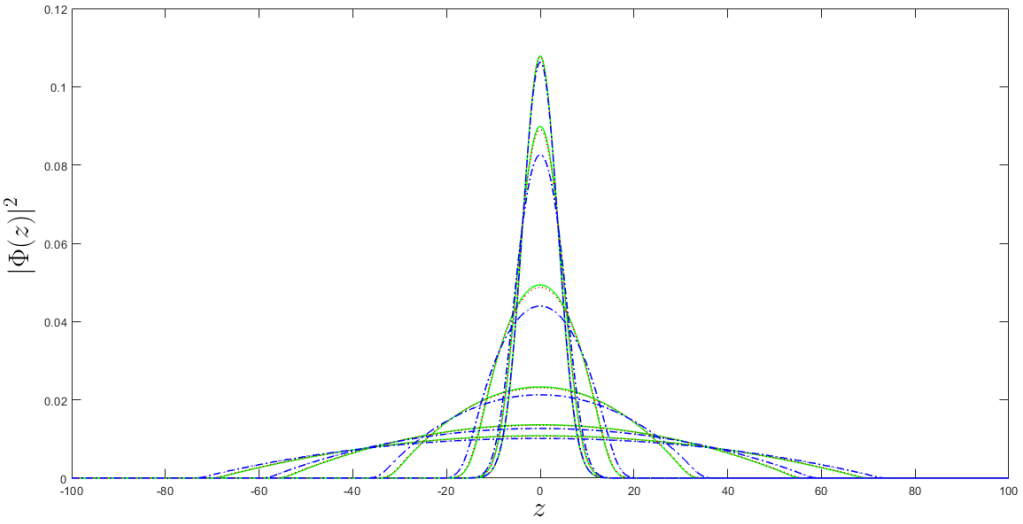

Figure 3.8: Sections of the dynamic evolution of the MGPE at $t = 5$ plotted all together with different g and g' terms.

The evolution of the Gaussian distribution towards a TF distribution as g grows is prominent in Figure 3.8.

Conclusions

The completion of this work has required four steps:

1. As a basic pre-requisite, we have had to acquaint ourselves with the physics of the Bose-Einstein Condensates and with their mathematical description by means of the Gross-Pitaevskii equation.

2. Next, we have developed analytically the MGPE (2.29) corresponding to a condensate in the ground state of the transverse trap and subsequently we have recast it into dimensionless form. To this effect, we have postulated a Gaussian form for the distribution of the transversal coordinates of the wave function for a cigar-shaped trapping potential, we have integrated over the transverse variables and further, we have derived the Euler-Lagrange equation for the appropriate action potential.

3. Then, we have performed extensive numerical simulations with the help of the GPELab toolbox of the MATLAB computing environment. Clearly, this task has necessitated the conduction of a preliminary study of the numerical methods employed to solve the nonlinear Schrödinger equation in both its stationary and dynamic regimes.

4. Finally, we have tried to uncover the subtle influence of the quantum fluctuating term with the help of the manifold numerical simulations that we have carried out.

Let us outline the main results of this work:

First, as stated previously in Step 2, we have achieved the reduction of equation (2.23) from 3D to 1D. This equation describes a condensate under strong transversal confinement and its main characteristic is the presence of a new quartic nonlinear term which describes the quantum fluctuation.

Second, we have performed an extensive array of numerical simulations in order to integrate the said nonlinear partial differential equation under the influence of different sets of parameters, both in the stationary and the dynamical regimes.

These performances have allowed us to observe the strong influence of the binary interatomic interaction term in the shape of the condensate: the density distribution of the BEC transitions from being Gaussian to being TF as the parameter g and thus, the number con atoms N, grow.

As a result, the simulations seem to indicate that the corrections of the quantum fluctuation term to the GPE based results may be as large as 10% when the conditions of the BEC are $g \approx g' \approx 10$.

Nevertheless, when the value of the g' coefficient is smaller than the value of the g coefficient, the corrections introduced by using the MGPE are very slight compared to the results given by the mean field approximation.

Appendix A

Numerical methods

The aim of this appendix is to present the numerical methods implemented in GPELab, the Matlab [32] third party toolbox that we have used for computing both the stationary state solutions and the dynamic evolution of the condensates [30, 31]. Recent research [33] has provided wide support as to its reliability and effectiveness.

A.1 Backward Euler pseudoSpectral (BESP) scheme

This next development follows section 4.1.2 of Ref. [30]. Different schemes for computing ground states are available. Here, we chose BESP for its high order accuracy [34]. This method is based on Backward Euler in time but on a Spectral Fast Fourier Transform scheme in space. Therefore, it considers an approach based on Fourier series representation through FFTs in order to calculate the derivatives in the backward Euler scheme. In the following we present the 1D version. Artificial periodic boundary conditions are imposed on the boundary of a computational box of length L assuming the solution is confined in it. Our spatial grid has J points, thus, the uniform discretization step h can be described as

$$h = (z_j - z_{j-1}) = \frac{2L}{J}. \tag{A.1}$$

The discrete Fourier pseudospectral disretization is given by

$$\Phi(z_j, t) = \frac{1}{J} \sum_{k=-J/2}^{J/2-1} \hat{\Phi}_k(t) e^{\frac{2\pi i k}{L} z_j}, \tag{A.2}$$

where $\hat{\Phi}_k(t)$ is the Fourier coefficient

$$\hat{\Phi}_k(t) = \sum_{j=0}^{J-1} \Phi(z_j, t)\, e^{-\frac{2\pi i k}{L} z_j}. \tag{A.3}$$

The spatial approximation for the Backward Euler scheme is

$$\frac{\Phi - \Phi^n}{\delta_t} = \frac{1}{2}\frac{\partial^2}{\partial z^2}\Phi - \frac{1}{2}\lambda z_j^2 \Phi - \beta|\Phi^n|^2\Phi - \alpha|\Phi^n|^3\Phi, \qquad \Phi^{n+1} = \frac{\Phi}{||\Phi||_0}. \tag{A.4}$$

By using the Fourier discrete transform, the second derivative of a function can be computed as such:

$$(\partial_z^2\Phi)_j = \frac{1}{J}\sum_{k=-J/2}^{J/2-1} -\mu_k^2\, \hat{\Phi}_k(t)\, e^{\frac{2\pi i k}{L} z_j}. \tag{A.5}$$

The discrete norm is given by

$$||\Phi||_0 = \sqrt{h_z}\sqrt{\sum_j |\Phi_j|^2}. \tag{A.6}$$

Now we must solve a nonlinear system at each iteration the stopping criterion being defined as

$$||\Phi^{n+1} - \Phi^n||_\infty < \varepsilon\, \delta t. \tag{A.7}$$

The chosen values for ε and δt are specified in Chapter 3.

A.2 Spectral scheme for simulating of the dynamics

This next development follows section 3.1.2 of Ref. [31]. First, lets recall the time-dependent dimensionless Modified Gross-Pitaevskii equation

$$\imath\, \frac{\partial \Phi}{\partial t} = \left[-\frac{1}{2}\partial_z^2\, \Phi + V + g\,|\Phi|^2 + g'\,|\Phi|^3\right]\Phi. \tag{A.8}$$

To observe the time evolution of the condensate we will remove the trapping potential by imposing $V = 0$.

A.2.1 Implicit-Time Splitting pseudoSPectral scheme

Let us define two operators, A and B and consider the following time dependent partial differential equation

$$\begin{cases} \partial_t \Phi(z,t) &= A\,\Phi(z,t) + B\,\Phi(z,t) \\ \Phi(z,0) &= \Phi_0(z). \end{cases} \tag{A.9}$$

The solution for $t > 0$ has the form $\Phi(z,t) = e^{(A+B)t}\,\Phi_0(z)$. The time-splitting schemes approximate the solution of Φ splitting the exponential operator $e^{(A+B)t}$ using the Trotter product formula [22]:

$$\Phi(z,t+\delta t) = e^{(A+B)t}\,\Phi(z,t) \approx e^{a_1 A\delta t}\,e^{b_1 B\delta t}\,e^{a_2 A\delta t}\,e^{b_2 B\delta t}...e^{a_n A\delta t}\,e^{b_n B\delta t}\,\Phi(z,t), \tag{A.10}$$

where $\{a_i, b_i\}_{1\leq i\leq n} \subset \mathbb{R}$ are computed weights to approximate $e^{(A+B)t}$. We will use the Strang scheme (which is of order two and unconditionally stable) where $a_1 = a_2 = 1/2$ and $b_1 = 1, b_2 = 0$.

Let us define the A and B operators as the following decomposition of our equation

$$A = \frac{\imath}{2}\,\partial_z^2, \qquad\qquad B = -\imath\, g\,|\Phi(z,t)|^2 - \imath\, g'\,|\Phi(z,t)|^3. \tag{A.11}$$

The partial differential equation associated to the operator A can be efficiently solved by using Fast Fourier Transforms (FFT) whereby the FT of a derivative becomes a multiplicative operator and the nonlinear ordinary differential equation associated to B can be integrated exactly.

Therefore, the approximation of the solution remains

$$\Phi(z,t+\delta t) \approx e^{\imath(1/2\partial_z^2)\delta t/2}\,e^{-\imath(g\,|\Phi|^2 + g'\,|\Phi|^3)\,\delta t/2}\,e^{\imath(1/2\partial_z^2)\delta t/2}\,\Phi(z,t). \tag{A.12}$$

Departing from the ground state solution we want to solve equation (A.8) on an uniformly discretized time-interval. We must start computing the solution of the PDE:

$$\begin{cases} \imath\partial_t \Phi_1(z,t) = -\partial_z^2 \Phi_1(z,t), t_n < t \leq t_{n+1/2} \\ \Phi_1(z,t_n) = \Phi^n(z). \end{cases} \tag{A.13}$$

This equation can be easily solved by inverting the second derivative operator through FFTs.

The next step is to determine the solution of the ODE:

$$\begin{cases} \imath\partial_t\Phi_2(z,t) = -g\,|\Phi_2(z,t)|^2\,\Phi_2(z,t) - g'\,|\Phi_2(z,t)|^3\,\Phi_2(z,t), t_n < t \leq t_{n+1/2} \\ \Phi_2(z,t_n) = \Phi_1(z,t_{n+1/2}), \end{cases} \tag{A.14}$$

whose solution is

$$\Phi_2(z,t) = \Phi_1(z,t_{n+1})\,e^{-\imath g\,|\Phi_1(z,t_{n+1})|^2\,(t-t_n) - \imath g'\,|\Phi_1(z,t_{n+1})|^3\,(t-t_n)}, \tag{A.15}$$

which finally gives: $\Phi^{n+1}(z) \approx \Phi_2(z,t_{n+1/2})$.

All these techniques and methods enable us to solve completely the problem of a freely expanding condensate.

Bibliography

[1] *Macroscopic quantum phenomena*, En.Wikipedia.Org, (2020).

[2] J. Emspak, *States of Matter: Bose-Einstein Condensate*, Livescience.Com (2018).

[3] W. Bao and Y. Cai, *Mathematical theory and numerical methods for Bose-Einstein condensation*, Kinetic & Related Models **6**, 3, (2013).

[4] A. Movilla, *Numerical simulation of the interference between two Bose-Einstein condensates*, University of the Basque Country, Final degree Thesis, (2016).

[5] J. Anglin and W. Ketterle, *Bose-Einstein condensation of atomic gases*, Nature **416**, 211, (2002).

[6] S. N. Bose, *Warmegleichgewicht im strahlungsfeld bei anwesenheit von materie*, Zeitschrift fur Physik A Hadrons and Nuclei **27**, 384, (1924).

[7] L. Galati and S. Zheng, *Numerical Solutions To The Gross-Pitaevskii Equation For Bose-Einstein Condensates*, Georgia Southern University, Electronic Theses and Dissertations **844**, (2013).

[8] A. Griffin, D. Snoke and S. Stringari, *Bose-Einstein condensation*, Cambridge University Press, (1996).

[9] F. London, *The λ-phenomenon of liquid helium and the Bose-Einstein degeneracy*, Nature **141**, 643, (1938).

[10] F. London, *On the Bose-Einstein Condensation*, Phys. Rev. **54**, 947, (1938).

[11] L. Salasnich, *Self-consistent derivation of the modified Gross-Pitaevskii equation with Lee-Huang-Yang correction*, Applied Sciences **8**, 10, (2018).

[12] C. E. Hecht, *The possible superfluid behaviour of hydrogen atom gases and liquids*, Physica **25**, 1159, (1959).

[13] I. F. Silvera and J. T. M. Walraven, *Stabilization of atomic Hydrogen at low temperature*, Phys. Rev. Lett. **44**, 164, (1980).

[14] F. Dalfovo, S. Giorgini, L. Pitaevskii and S. Stringari, *Theory of Bose-Einstein condensation in trapped gases*, Reviews Of Modern Physics **71**, 463,(1999).

[15] M. H. Anderson, J. R. Ensher, M. R. Matthewa, C. E. Wieman and E. A. Cornell, *Observation of Bose-Einstein condensation in a dilute atomic vapor*, Science **269**, 198, (1995).

[16] K. B. Davis, M. O. Mewes, M. R. Andrews, N. J. van Druten, D. S. Durfee, D. M. Kurn and W. Ketterle, *Bose-Einstein condensation in a gas of sodium atoms*, Phys. Rev. Lett. **75**, 3969 (1995).

[17] C. C. Bradley, C. A. Sackett, J. J. Tollett and R. G. Hulet,*Evidence of Bose-Einstein condensation in an atomic gas with attractive interaction*, Phys. Rev. Lett. **75**, 1687 (1995).

[18] D. G. Fried, T. C. Killian, L. Willmann, D. Landhuis, S. C. Moss, D. Kleppner and T. J. Greytak, *Bose-Einstein condensation of atomic hydrogen*, Phys. Rev. Lett.**81**, 3811, (1998).

[19] A. J. Leggett, *Bose-Einstein condensation in the alkali gases: Some fundamental concepts*, Rev. Mod. Phys. **73**, 307, (2001).

[20] E. P. Gross, *Structure of a quantized vortex in boson systems*, Nuovo Cimento **20**, 454, (1961).

[21] L. P. Pitaevskii, *Vortex Lines in an Imperfect Bose Gas*, Sov. Phys. **13**, 451, (1961).

[22] M. Modugno, *An introduction to the theory of Bose-Einstein condensation in trapped gases*, Lecture notes, (2016).

[23] E. H. Lieb, R. Seiringer, J. P. Solovej and J. Yngvason, *The Mathematics of the Bose Gas and its Condensation*, Oberwolfach Seminars **34**, (2005).

[24] L. P. Pitaevskii and S. Stringari, *Bose-Einstein Condensation*, Clarendon Press, Oxford, (2003).

[25] E. Braaten and A. Nieto, *Quantum Corrections to the Ground State of a Trapped Bose-Einstein Condensate*, Physical Review **56**, (1997).

[26] A. Fabrocini and A. Polls, *Bose-Einstein condensates in the large-gas-parameter regime*, Physical Review A **64** 063610, (2001).

[27] L. Salasnich, A. Parola and L. Reatto, *Effective wave-equations for the dynamics of cigar-shaped and disc-shaped Bose condensates*, Physical Review A **65**, (2002).

[28] W. Cardoso, A. Avelar and D. Bazeia, *One-dimensional reduction of the three-dimenstional Gross-Pitaevskii equation with two- and three-body interactions*, Physical Review E **83**, (2011).

[29] S. Adhikari and L. Salasnich, *Effective nonlinear Schrödinger equations for cigar-shaped and disc-shaped Fermi superfluids at unitarity*, New Journal Of Physics **11**, (2009).

[30] X. Antoine and R. Duboscq, *GPELab, a Matlab toolbox to solve Gross–Pitaevskii equations I: Computation of stationary solutions*, Computer Physics Communications **185**, (2014).

[31] X. Antoine and R. Duboscq, *GPELab, a Matlab toolbox to solve Gross–Pitaevskii equations II: Dynamics and stochastic simulations*, Computer Physics Communications **193**, (2015).

[32] Mathworks.com (2020).

[33] M. Pijoan, R. Bahí and P. Mestres *Numerical Methods for the study of Bose-Einstein Condensates using the Gross-Pitaevskii Equation*, Universidad Politécnica de Cataluña, 187708, (2019).

[34] X. Antoine and R. Duboscq, *Modeling and computation of Bose-Einstein condensates: stationary states, nucleation, dynamics, stochasticity*, Lecture notes in Mathematics, Springer, (2014).